



ELSEVIER

Contents lists available at ScienceDirect

Optics Communications

journal homepage: www.elsevier.com/locate/optcom

Performance investigation on clipping and RIN induced degradation for a single- and two-tone IM-DD SCM optical link

Gausia Qazi ^{a,*}, Ajay K. Sharma ^b, H. Najeeb-ud-din Shah (SMIEEE) ^a, Moin Uddin ^c

^a Department of Electronics and Communication Engineering, National Institute of Technology Srinagar, 190006, Jammu and Kashmir, India

^b National Institute of Technology Delhi, India

^c Professor, Jamia Hamdard University, New Delhi, India

ARTICLE INFO

Article history:

Received 15 July 2013

Received in revised form

4 December 2013

Accepted 23 December 2013

Available online 18 January 2014

Keywords:

Clipping

HD

IMD

Radio-over-fiber (RoF)

RIN

SCM

ABSTRACT

Subcarrier multiplexing (SCM) is preferred multiplexing approach for its simplicity and cost effectiveness in optical broadband transmission. In this work four basic SCM based intensity modulation direct detection (IM-DD) systems models have been devised to investigate laser source induced noise mechanisms. These system models reveal unique spectral behavioural characteristics associated to harmonic distortion (HD), inter-modulation distortion (IMD), clipping and random intensity noise (RIN) mechanisms. Response of clipping and RIN mechanisms to changes in system operational and laser design parameters show a direct dependence of clipping spillover on modulation current and an insensitivity of the RIN spectrum to changes in carrier amplitude. High bias currents are shown to reduce negative influence of clipping and RIN peak power while shifting RIN peak above subcarrier operating range of frequencies but increases RIN spectrum width. Low laser quantum efficiency is observed to favor clipping and RIN induced distortion while RIN peak position is insensitive to laser quantum efficiency. With active layer volume there will exist a tradeoff between clipping spillover and RIN peak power on one hand and RIN peak position and RIN spectral width on the other hand. High laser carrier lifetime will favor clipping spillover reduction. All the results so obtained can be exploited for identifying a suitable laser design in a suitable system model for achieving better system performance for the SCM based IM-DD systems.

© 2014 Elsevier B.V. All rights reserved.

1. Introduction

Optical fiber has become a transmission medium of choice as it offers virtually unlimited and an unregulated bandwidth to the end users, yet its potential bandwidth remains poorly exploited. The high bandwidth and low attenuation feature of this transmission medium makes it suitable for high capacity backbone networks [1,2]. Subcarrier multiplexing (SCM) is a preferred multiplexing technique used to tap the enormous bandwidth of an optical fiber efficiently because of its simplicity, versatility and cost effectiveness in broadband delivery to the end users. It uses microwave devices like the RF oscillators which are much more mature, readily available, and highly stable and sensitive in comparison to their optical counterparts and allows allocation of closely spaced channels over several GHz on the optical spectrum [2–4]. SCM has many variants ranging from its use in non-fiber all radio frequency (RF) communication to its convergence into optical domain as in radio over fiber (RoF) [5–8]. This system integrates the complementary

transmission media of radio and light waves. It facilitates easy access and high mobility over the large bandwidth of the optical medium. The detected RF subcarriers can be distributed to home subscribers or radiated to mobile terminals or fixed terminals like in cellular communication networks. Another typical application of SCM technology in fiber optic system is analogue cable television (CATV) distribution over a hybrid fiber-coaxial network (HFC) advancing from simple one-way broadcasts to two-way simultaneous analogue and digital broadband service delivery [3,4,9,10].

In an SCM based intensity modulation-direct detection (IM-DD) system, direct modulation of a laser is much simpler and economical solution than implementing external modulation [9]. External modulators ensure better performance but at the cost of insertion loss penalty [11]. However the most serious disadvantage of direct modulation technique are limited bandwidth (about 10 GHz) and limited SNR by high chirp and inherent laser nonlinearities namely inter-modulation distortion (IMD) and random intensity noise (RIN) [6,8,9]. Clipping is one of the factors that affect the carrier to noise ratio (CNR) and system performance besides IMD [4,9,11]. The consequence of operation of lasers near its threshold results in IMD [3] as well as clipping induced degradation. Laser non-linearity and large optical modulation depth results in unacceptable levels of IMD

* Corresponding author. Mob.: + 91 9419015436.
E-mail address: gausia.qazi@yahoo.com (G. Qazi).

[12,13]. In case of the SCM based multi-carrier systems clipping is a major limiting factor due to the wide signal variations of the multiplexed signals and also limits the number of simultaneously active users [14]. The allowed modulation depths is limited by clipping in SCM based CATV systems in which care has been taken to eliminate lasers sub-linearity [9,15]. Linearity, RIN and modulation efficiency are important laser characteristics for analogue links that limit the dynamic range, gain and noise figures of fibre optical link [5]. The constraints imposed by noise and nonlinearities have to be understood for an appropriate solution for these systems.

In this work carriers are fed to SCM based IM-DD system to investigate its laser source as a noise contributor of RIN due to its non-ideal behaviour and clipping noise due to its operation near its specified threshold current value. In this work four basic models have been devised for studying the spectral behavioural characteristics of clipping and RIN noise mechanisms and their impact on HD and IMD and to observe the influence of each of these laser originating impairments on the detected spectrum individually. Their response to key system operational and design parameters has been investigated to identify possible corrective measures for reasonable suppression of these mechanisms. In Section 2 several aspects of RIN and clipping noise mechanisms in an SCM based IM-DD environment and the various solutions implemented for performance improvement have been discussed. Section 3 gives the description of a single-and two-tone SCM based IM-DD system designed using a laser rate equation component as a directly modulated laser source. Four system models will be identified thereby to carry out the investigations. The results and discussion are highlighted in Section 4 while the conclusion and future scope is presented in Section 5.

2. Non-ideal laser diode behaviour

The most serious problem in SCM systems is the source non-linearity [2,5,14,15] where lasing power changes non-linearly with injection current. This non-ideal laser diode behaviour is attributed to carrier heating effects [15] and the interaction of electrons and photons during stimulated recombination process [11,12]. Resulting noise and distortion mechanisms attain their peak at the laser resonant frequency [3,5,12]. In broadcast environment when current modulation of a nonlinear laser source contains several sub-frequencies there will be mixing between different subcarriers producing IMD in addition to their harmonics due to HD [3,5,7]. The laser source is also a noise contributor of RIN due to its non-ideal behaviour and clipping noise due to its operation near its specified threshold current value [5,6,16].

Even if laser light versus current characteristics are made perfectly linear and resonant frequency extended to infinity, yet the allowed modulation depths is limited by clipping if laser is driven (biased) near or below threshold current value. Clipping occurs when the total modulation currents drop into the non-conducting region of the laser and limits the peak performance in BER [14].

System performance degradation due to laser nonlinear behaviour is more severe in an analogue than in digital modulation applications while influence of clipping is more apparent in AM-VSB in systems where the laser L-I characteristics are made perfectly linear and the resonance distortion (RD) is eliminated [9]. In the subcarrier transmission of multichannel AM-VSB signals in video distribution system, limitations are imposed by the laser nonlinearity and noise and strict linearity requirements arise from the NTSC standard video format used. Although AM-VSB system minimize the required bandwidth on one hand, however in exchange to avoid the degradation in the picture quality the required CNR must be between

45 to 55 dB. Comparatively both FM and digital video require a lesser CNR of 20 dB for the acceptable picture quality [5,9].

It has been shown [9,16] that the total carrier to interference ratio (CIR) resulting from clipping is given by

$$\text{CIR} = \frac{(2\pi)^{1/2}(1+6\mu^2)\exp(\mu^2/2)}{\mu^3} \quad (1)$$

where $\mu = m(N/2)^{1/2}$ and N is the number of SCM channels and m is modulation index per channel forming a basis for investigation of carrier-to-interference ratio as a function of modulation index per channel (m) for AM-VSB systems. It is observed that CNR is limited by quantum limit (shot noise only) for small m and by clipping for large m [9]. Similarly clipping induced distortion causes degradation in case of short trunk AM-VSB/M-QAM light wave system when the laser is driven below composite AM/QAM signal resulting in clipping modulated waveforms [10]. Clipping also causes significant spectral leak into adjacent channels and filtering has been proposed to reduce the adjacent channel interference but this causes peak re-growth [5]. Another solution proposed is that of pre-clipping an analogue signal before modulation by limiter [10].

Random intensity noise (RIN) also originates at the laser source and is generated by spontaneous emission or caused by coherency within the laser even in the absence of current modulation. The source RIN contribution to the noise current at the detector is expressed as [16]

$$\langle \text{IRIN} \rangle = I^2 \times \text{RIN} \times B \quad (2)$$

where I is the photo current, RIN noise power spectral density is defined as the ratio of mean square of intensity fluctuation δ_p to the square of mean intensity P given by

$$\text{RIN} = \frac{\langle \delta_p^2 \rangle}{P^2} \quad (3)$$

In SM operations RIN is almost constant at lower RF frequencies where as it peaks at resonance [4,16]. RIN can increase by 10 to 20 dB in the presence of back reflected signals. This demands the use of low feedback connectors or optical isolators to minimize RIN [4]. The SCM systems, which use robust modulation format like FM or digital systems and where detected photocurrent at receiver are small, are less susceptible to impairments from RIN. For any type of system RIN of -102 dB/Hz is unacceptable. Good diode lasers have RIN of -160 dB/Hz or better [9]. Feed forward technique to suppress IMD also help in reducing laser intensity noise, but suffers from techno-economical drawback, higher cost and higher complexity [13]. Higher output power gives low RIN [16] and impact of RIN can be reduced by using laser sources with smaller line widths [6].

Better performance can be made possible by way of selecting appropriate operational frequencies. Since noise and distortion mechanisms attain their peak at the laser resonant frequency [4,5] thus the usable bandwidth of SCM systems should be favourably limited to low frequencies [5] where high linearity is achievable [9] and where mature, readily available and relatively inexpensive electronic fabrication is possible. Low frequencies however are dominated by adverse influence of increased heating effect [3,15]. To increase the usable bandwidth, the resonant frequency can be shifted to higher frequencies well above subcarrier frequencies by allowing sufficiently large bias current values through the laser diode [17].

3. Simulation setup of basic IM-DD SCM system

A back to back arrangement of a basic IM-DD SCM system was designed based on the laser rate equation component [18,19] of the simulator [20] as shown in Fig. 1(a) followed by an illustration

of the simulation flowchart as shown in Fig. 1(b). The laser rate equation component has been used to simulate the modulation dynamics of a laser which has been intensity modulated by carriers f_1 and f_2 equal to 500 and 525 MHz, respectively. At the receiver the received optical signal is detected by a PIN detector. The RF spectral analyzer is used to observe the RF spectrum of the detected signal. The electrical carrier analyzer is used to measure the power of the clipping and RIN induced distortion components. The distortion is observable in the detected signal on the CRO display. These investigations enable to identify the most influencing signal, operational and device parameters which can be exploited to effectively suppress these mechanisms. Four basic

system models namely clipping disabled-RIN disabled (CD-RD), clipping enabled-RIN disabled (CE-RD), clipping disabled-RIN enabled (CD-RE) and a clipping enabled-RIN enabled (CE-RE) have been devised using the basic IM-DD system of Fig. 1(a) with laser power equal to 0 dBm. The threshold current I_{th} is equal 33.46 mA and threshold power is equal to 0.028 mW unless otherwise specified. To realize these system models the parameters listed in the following Table 1(a)–(d) are used.

The clipping enabled-RIN disabled and clipping enabled-RIN enabled IM-DD models have been realized by operating a laser source at low bias current so that product of carrier amplitude A and I_{pk} is greater than difference of I_{bias} and I_{th} where the RIN in

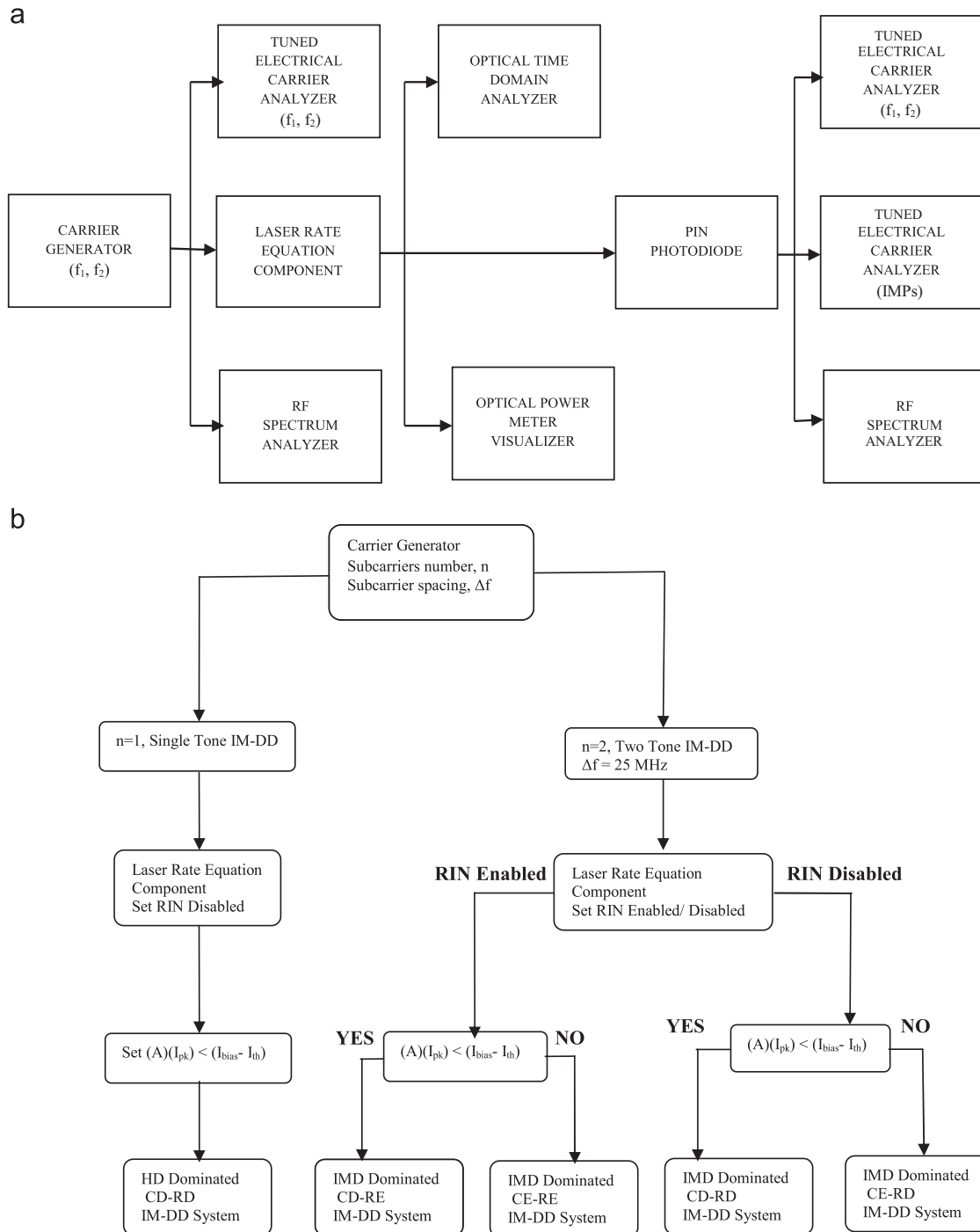


Fig. 1. (a) Basic simulation setup of a typical single-tone and a two-tone IM-DD SCM system having single-tone (f_1) transmitter/single-tone (HD) receiver/two-tone (f_1, f_2) SCM transmitter/two-tone (HD AND IMP) receiver; (b) simulation flowchart based on Laser rate equation component as the active laser source to realize IM-DD SCM system models.

laser is disabled in the former and is enabled in the later. Similarly when laser is operated with high bias current so that the product of A and I_{pk} is less than the difference between I_{bias} and I_{th} and RIN in laser is enabled or disabled then the models so devised are Clipping Disabled-RIN Enabled and Clipping Disabled-RIN Disabled system model, respectively.

The laser rate equation component used in the simulation is based on single mode formulation of carrier density rate equation and the photon density rate equation [18,19] given by Eqs. (4a) and (4b), respectively.

$$\frac{dN(t)}{dt} = \frac{I(t)}{qV} - \frac{N(t)}{\tau_n} + g_0 \frac{[N(t) - N_t]}{[1 + \varepsilon S(t)]} S(t) \quad (4a)$$

$$\frac{dS(t)}{dt} = \Gamma \beta \frac{N(t)}{\tau_n} - \frac{S(t)}{\tau_p} + \Gamma g_0 \frac{[N(t) - N_t]}{[1 + \varepsilon S(t)]} S(t) \quad (4b)$$

here $N(t)$ is the electrons carrier density (cm^{-3}); $I(t)/qV$ is the total injected electron rate ($\text{amp cm}^{-1} \text{cm}^{-3}$); V is the active layer volume (cm^3); τ_n is the carrier life time (s); g_0 is the differential gain coefficient (cm^2); N_t is carrier density at transparency (cm^{-3}); $S(t)$ is the photon density (cm^{-3}); ε is the gain compression coefficient (cm^3); Γ is the optical mode confinement factor; β is the spontaneous emission factor; and τ_p is the photon life time (s).

4. Results and discussion

In this work investigations have been carried out on the four basic afore mentioned IM-DD system models for studying their spectral behavioural characteristics. Additionally these models have been used to study the sensitivity of Clipping mechanism and RIN Spectrum to changes in key operational and system device parameters and to study their impact on HD and IMD mechanisms.

4.1. Spectral response of IM-DD system models

The spectral displays of the four systems models described above are shown in Fig. 2(a)–(e). RF spectrum display of four basic IM-DD system models devised reveals distinct unique characteristics in the spectral domain that can be associated with the various impairment mechanisms influencing the respective system. A single carrier of 1.5 au and at frequency of 500 MHz is fed to Clipping Disabled-RIN Disabled system designed as per specifications in Table 1(a). The resulting spectrum of Fig. 2(a) shows HD induced components while IMD, clipping and RIN influence are absent from the spectrum. The power of these harmonics becomes insignificant at higher spectral position on the spectrum. On the contrary, in the same system of Table 1(a), when two subcarriers at 500 and 525 MHz frequencies mix in the nonlinear laser source

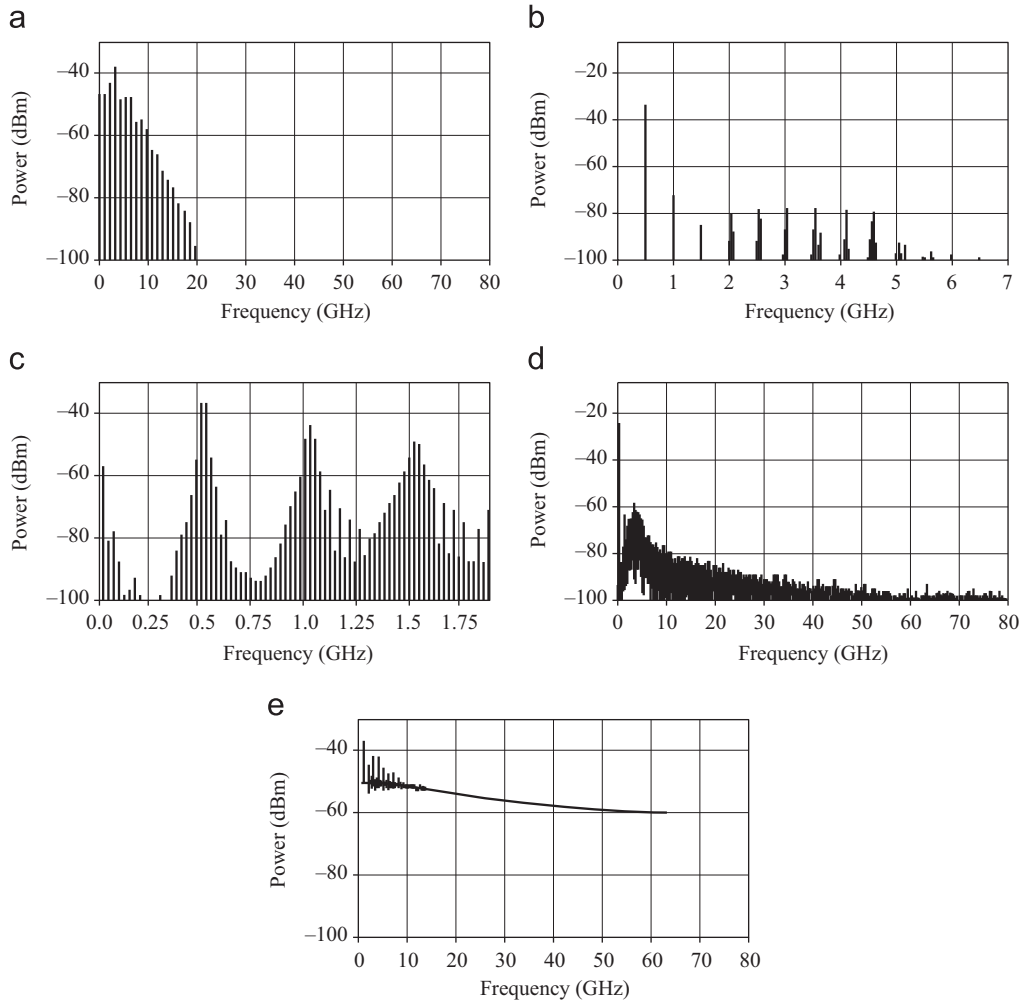


Fig. 2. RF spectrum display of four basic IM-DD models; (a) single-tone clipping disabled-RIN disabled system where $A = 1.5$ au; $I_{bias} = 50$ mA; (b) two-tone clipping disabled-RIN disabled system where $A = 0.25$ au; $I_{bias} = 50$ mA; (c) two-tone clipping enabled-RIN disabled where $A = 1.5$ au; $I_{bias} = 38$ mA; (d) two-tone clipping disabled-RIN enabled system where $A = 1.5$ au; $I_{bias} = 50$ mA; (e) two-tone clipping enabled-RIN enabled system where $A = 1.5$ au; $I_{bias} = 38$ mA.

Table 1

The parameter values used for designing (a) clipping disabled–RIN disabled, (b) clipping enabled–RIN disabled, (c) clipping disabled–RIN enabled, and (d) clipping enabled–RIN enabled IM-DD system models.

Parameter name	Parameter value
Modulation peak current (I_{pk})	3.8 mA
Laser quantum efficiency	0.4
Laser active layer volume (V)	$1.5E-10 \text{ cm}^3$
Laser carrier life time (τ_n)	$1E-009 \text{ s}$
Laser photon life time (τ_p)	$3E-012 \text{ s}$
Laser spontaneous emission factor (β)	$3E-005$
Laser gain compression coefficient (ϵ)	$1E-017 \text{ cm}^3$
Transparency carrier density (N_t)	$1E+018 \text{ cm}^{-3}$
(a) Clipping disabled–RIN disabled system model	
Single-tone carrier amplitude (A)	1.5 a.u
Two-tone carrier amplitude (A)	0.25 a.u
Bias current (I_{bias})	50 mA
Clipping mechanism disabled	(A) (I_{pk}) less than ($I_{bias}-I_{th}$)
RIN in laser	Disabled
(b) Clipping enabled–RIN disabled system model	
Two-tone carrier amplitude (A)	1.5 au
Bias current (I_{bias})	38 mA
Clipping mechanism enabled	(A) (I_{pk}) greater than ($I_{bias}-I_{th}$)
RIN in laser	Disabled
(c) Clipping disabled–RIN enabled system model	
Two-tone carrier amplitude (A)	1.5 au
Bias current (I_{bias})	50 mA
Clipping mechanism disabled	(A) (I_{pk}) less than ($I_{bias}-I_{th}$)
RIN in laser	Enabled
(d) Clipping enabled–RIN enabled system model	
Two-tone carrier amplitude (A)	1.5 au
Bias current (I_{bias})	38 mA
Clipping mechanism enabled	(A) (I_{pk}) greater than ($I_{bias}-I_{th}$)
RIN in laser	Enabled

the resulting spectrum of detected signal shown in Fig. 2 (b) reveals the original carriers accompanied by clustered groups of IMPs. The IMD induced components seen are the second-order IMD components at 1000, 1025 and 1050 MHz; two-tone third-order IMD components at 1525 and 1550 MHz; triple-beat third-order IMD components at 2025, 2050, and 2075 MHz and harmonics of 500 and 525 MHz. Again here spectrum does not show any influence of clipping and RIN mechanisms while HD mechanism is suppressed due to small carrier amplitude. In a two-tone clipping enabled–RIN disabled IM-DD system developed as per the specifications of Table 1(b), clipping mechanism is enforced because the product of A and I_{pk} exceeds the difference between I_{bias} and I_{th} . The corresponding RF spectrum analyzer display of Fig. 2(c) shows a peculiar clipping induced spectrum spillover or spectrum spread of the IMPs and their harmonics, when the laser is operated close to the clipping threshold limit. The spectrum in Fig. 2(d) of a Clipping Disabled–RIN Enabled system model based on specifications given in Table 1(c) shows the influence of RIN mechanism originating at the laser as a RIN induced spectrum with a typical RIN peak. Also HD and IMD mechanisms are induced in such a system when two subcarriers of amplitude 1.5 au pass through the nonlinear laser generating their harmonics and IMPs due to their mixing. The harmonics and IMPs are clearly observable riding atop the RIN spectrum. The RIN peaks at the resonant frequency. The spectrum of Fig. 2(e) based on the system model specified in Table 1(d) is similar to Fig. 2(d) as it also shows the RIN induced spectrum with the Harmonics and IMPs. However since in this system clipping is enabled thus the clipping induced spectrum spillover of the harmonics and IMPs is observed riding on top of the RIN spectrum. Further as this is the spectrum of a clipping enabled and RIN enabled IM-DD system, the different non linearity mechanisms will be highly empowered. Thus the increase in the noise floor.

4.2. Clipping induced performance degradation

The response of the clipping induced distortions in a clipping enabled–RIN disabled system has been investigated with respect to modulation peak current, laser bias current, laser quantum efficiency, laser active layer volume and carrier life time. In the following case studies carrier amplitude A and I_{pk} are equal to 0.25 au and 40 mA respectively and the other parameters used are as listed in Table 1(b). Clipping distortion results in the broadening of the linewidth which cause spectrum spillover as observed in the spectrum displayed in Fig. 2(c).

The clipping induced linewidth broadening is referred to as the clipping induced RF spectrum spread in this paper which is measured by monitoring the spectral position of a clipping induced distortion component by setting the bound to a reduced power of about -97 dBm [3]. Higher the spectral position of such a distortion component, more prominent will be the clipping induced spillover. The trends exhibited by results so obtained are a close approximation to the clipping induced full width half maximum (FWHM) linewidth measurements.

4.2.1. Clipping response to modulation peak current

A clipping enabled–RIN disabled system has been made clipping dominant by suppressing HD and IMD mechanisms by using a single carrier of a low amplitude equal to 0.25 au. The response of clipping mechanism is observed with respect to I_{peak} over a range 18.17 to 40 mA in Fig. 3. Over this range product of A and I_{pk} exceeds the difference offset of 4.54 mA between I_{bias} and I_{th} . The observations made show a direct relationship between the clipping induced RF spectrum spread and the input modulation peak

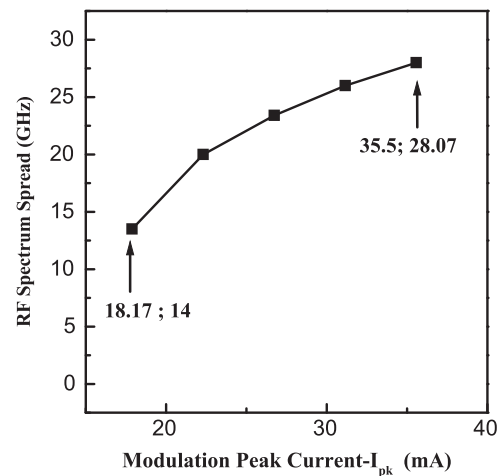


Fig. 3. Clipping induced RF spectrum spread vs. I_{pk} over range 18 to 40 mA.

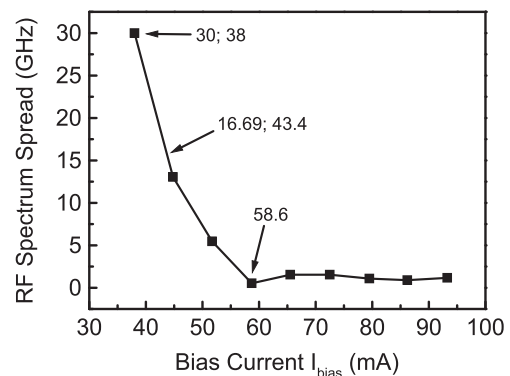


Fig. 4. Clipping induced RF spectrum spread vs. I_{bias} range from 38 to 100 mA.

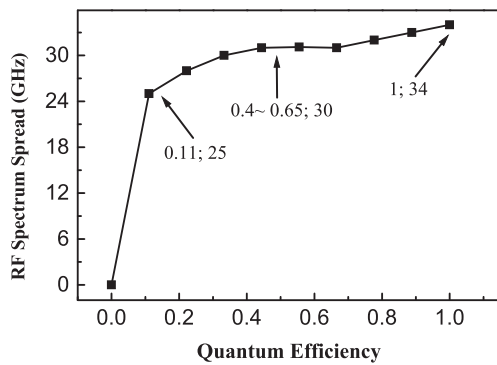


Fig. 5. Clipping induced RF spectrum spread against quantum efficiency range 0 to 1.

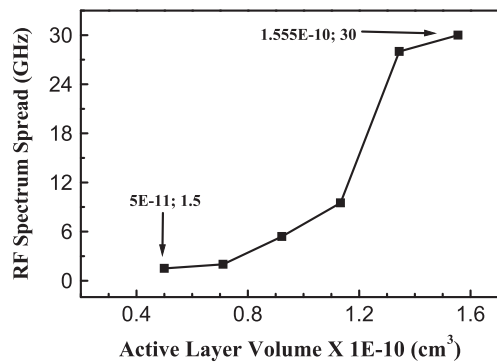


Fig. 6. Clipping induced RF spectrum spread against active layer volume range $5E-11$ to $1.555E-10$ cm^3 and minimum spillover of about 1.5 GHz to a maximum of about 30 GHz.

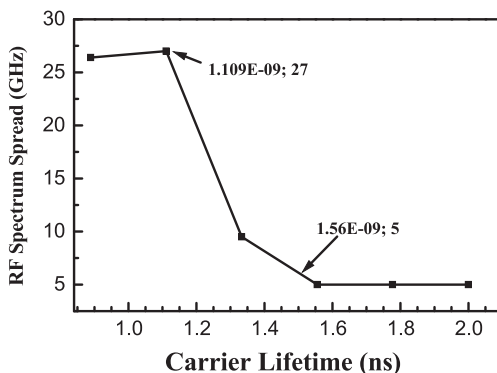


Fig. 7. Clipping induced RF spectrum spread against carrier lifetime range $8.889E-10$ to $2E-9$ s.

current (I_{pk}). The clipping induced spectrum spreads out gradually from about 14 GHz at 18.17 mA to 28.07 GHz at 35.5 mA.

4.2.2. Clipping response to laser bias current

Subsequently the experiment is repeated with respect to changes in I_{bias} varied from 38 to 100 mA and results are shown in Fig. 4. The system remains clipping enabled over I_{bias} range of 38 to 43.4 mA and above this current value the laser operation shifts well above the clipping threshold limit. The spectrum spillover reduces sharply from 30 GHz at a bias current of 38 mA to around 16.69 GHz at about 43.4 mA in the clipping enabled system. With further increase in laser bias current the clipping is overcome and clipping induced RF spread reduced around 0 GHz. The results here show an inverse dependence of clipping induced RF spread on the laser bias current with a steep slope gradient.

4.2.3. Clipping response to laser quantum efficiency

Clipping response to changes in laser quantum efficiency is shown in Fig. 5 when the laser quantum efficiency is varied from 0 to 1. The RF spectrum spreads out gradually with rise in quantum efficiency. It is also observed that an increase in spectrum spillover of just 9 GHz occurs over quantum efficiency range of 0.11 to 1.0, whereas from 0.4 to 0.65 spillover remains constant around 30 GHz. These results reveal a low sensitivity of clipping mechanism to changes in quantum efficiency.

4.2.4. Clipping response to laser active layer volume

The results of RF spectrum spread with respect to laser active layer volume are plotted in Fig. 6 which shows a sharp rise in the spillover observed with increase in active layer volume over range $5E-11$ to $1.555E-10$ cm^3 . Over this range the system suffers a minimum spillover of about 2 GHz to a maximum of about 30 GHz.

4.2.5. Clipping response to laser carrier lifetime

The results are plotted in Fig. 7 between clipping induced RF spectrum spread and laser carrier life time. The spectrum spread bears a sharp inverse relationship to the laser carrier lifetime. Over the carrier lifetime range from $1.109E-09$ to $1.56E-09$ s. the spillover decreases sharply from maximum of about 27 GHz till it remains constant around 5 GHz exhibiting a negative slope gradient. In the laser rate Eq. (4b), carrier depletion rate due to spontaneous emission is governed by $N(t)/\text{carrier life time}$. At low carrier life time the spontaneous emission is a dominant mechanism due to high recombination coefficients and hence the threshold current, which is dependent on laser physical parameters, assumes values close to the fixed laser bias current, thereby leading to clipping enhancement. Thus the broadened RF spectrum spread is attributed to clipping enhancement that would result in materials with small carrier life time. On the contrary, for materials with large carrier life time the recombination coefficient is low thereby rendering stimulated emission as the dominant mechanism. The threshold current is effectively reduced to lower power levels than the bias current. This reduces the influence of clipping and hence the RF spectrum spread also reduces till reasonable immunity towards clipping is achieved at high carrier life time.

4.3. RIN induced performance degradation

To investigate the influence of laser originating RIN on an IM-DD system, the Clipping Disabled-RIN Enabled system of Table 1 (c) was simulated with a single carrier selected of small carrier amplitude equal to 0.001 au so that the system is not influenced by HD and IMD. The RIN induced spectrum, its peak amplitude and its spectral width is studied with respect to changes in carrier amplitude, laser bias current, laser quantum efficiency, laser active layer volume and carrier lifetime. The RIN spectral width is a measure of RIN induced linewidth broadening adopted in this paper by monitoring the reduction in the spectrum power by setting the bound to a reduced power of about -97 dBm [3]. The measurements so obtained were observed to exhibit the same trend in close agreement to FWHM linewidth measurements. The RIN spectrum does not show any sensitivity to changes in carrier amplitude and also RIN does not show any such curve that could be interpreted with respect to carrier lifetime. The system has been simulated to see the sensitivity of the IM-DD system towards RIN inflicted degradation for all cases with a fixed carrier life time of 1.0 ns.

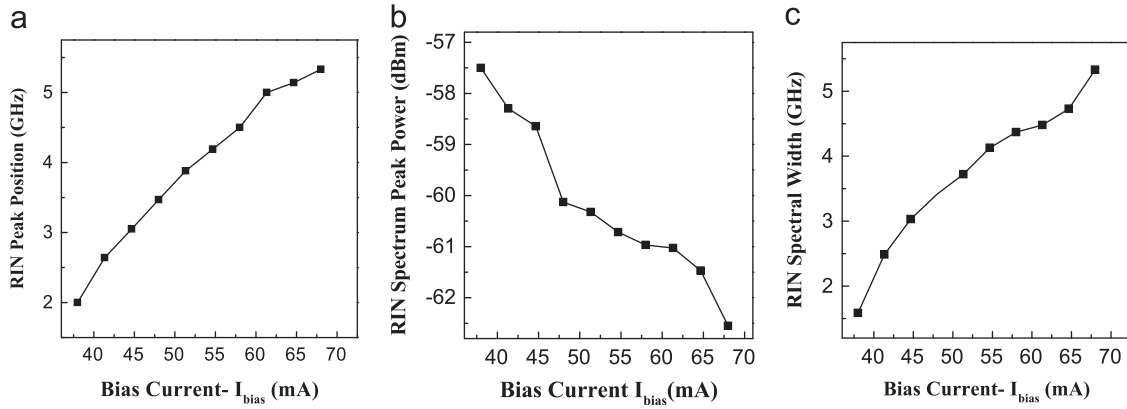


Fig. 8. RIN (a) spectrum peak position; (b) spectrum peak power, and (c) spectral width; vs. laser bias current.

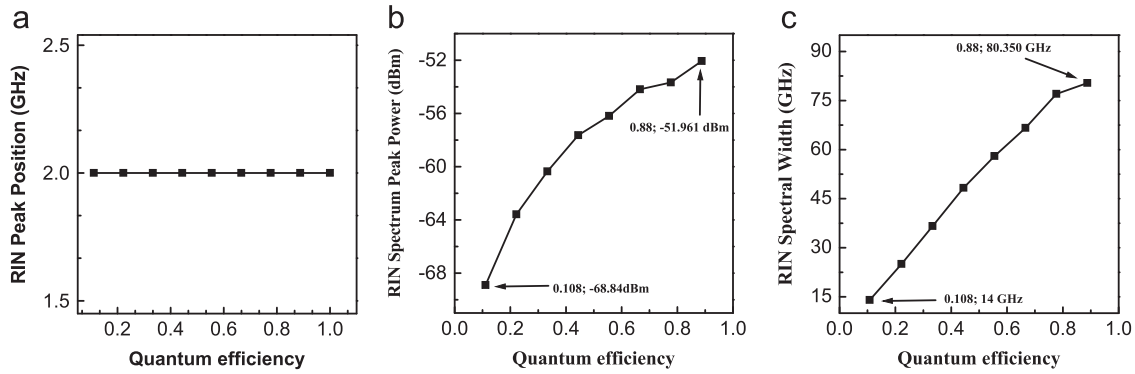


Fig. 9. RIN (a) spectrum peak position, (b) spectrum peak power, and (c) spectral width; vs. laser quantum efficiency.

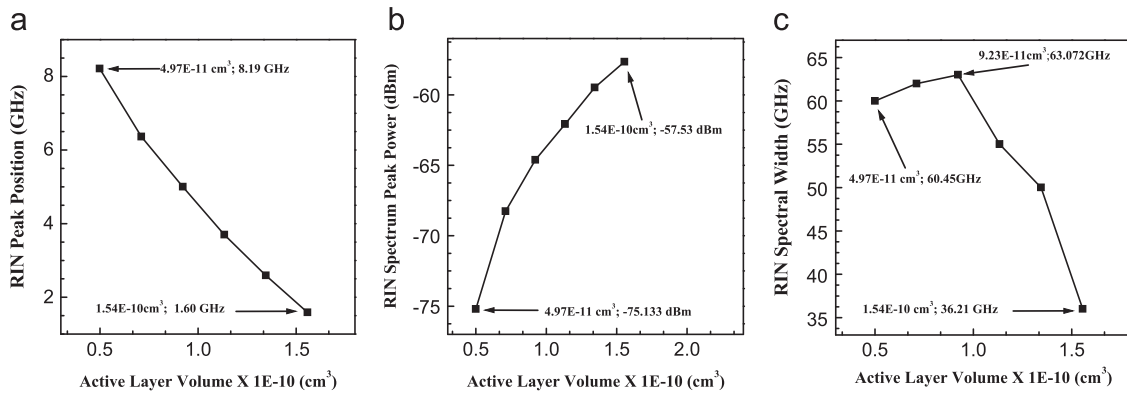


Fig. 10. RIN (a) spectrum peak position, (b) spectrum peak power, and (c) spectral width vs. active layer volume.

4.3.1. RIN response to laser bias current

In the single-tone RIN dominated IM-DD system, I_{bias} is varied from 38 to 68 mA. As RIN originates at the laser, changes in the bias current flowing through the source significantly influence the RIN spectrum as shown in Fig. 8(a)–(c). These figures show a non-linear direct dependence of RIN peak position and RIN spectral width with respect to laser bias current whereas a non-linear inverse dependence of RIN spectrum peak power on laser bias current, respectively.

4.3.2. RIN response to laser quantum efficiency

For the one carrier IM-DD system when the laser is biased at 38 mA the RIN peak appears at 2 GHz and the laser quantum efficiency is varied from 0.0 to 1.0. It is observed that the spectral

position of the RIN peak is completely insensitive to changes in laser quantum efficiency as shown in Fig. 9(a) whereas Fig. 9 (b) and (c) show sensitivity of RIN mechanism to quantum efficiency. The RIN spectrum peak power and its spectral width bear a direct relationship with respect to laser quantum efficiency which is linear in former and parabolic in latter. RIN spectral width increases from 14.29 to 80.350 GHz and RIN spectrum peak power increases from -68.84 to -51.961 dBm when observed over the quantum efficiency range from 0.108 to 0.88.

4.3.3. RIN response to active layer volume

On varying laser active layer volume from $4.95E-11$ to $1.555E-10$ cm^3 , the RIN spectrum peak position, its peak power and RIN

spectral width also changes as exhibited by Fig. 10(a)–(c). RIN peak position decreases sharply from 8.19 GHz at an active layer volume of $4.9\text{E} - 11\text{ cm}^3$ to 1.60 GHz at an active layer volume of $1.54\text{E} - 10\text{ cm}^3$. RIN spectrum peak power increases sharply from -75.13 dBm at an active layer volume of $4.9\text{E} - 11\text{ cm}^3$ to -57.53 dBm at $1.54\text{E} - 10\text{ cm}^3$. RIN spectrum spread is 60.45 GHz, then increases to 63.07 GHz and reduces to 36.21 GHz at active layer volumes equal to $4.9\text{E} - 11$, $9.23\text{E} - 11$ and $1.54\text{E} - 10\text{ cm}^3$, respectively.

On the basis of either theory [21] or measurements made in this paper, the threshold current increases with increase in the active layer volume. This indicates a RIN enhancement due to an increase in spontaneous emission as active layer volume increases. This RIN enhancement is reflected in the elevation of the RIN spectrum peak power where spontaneous emission is the predominant mechanism for large threshold current at large values of active layer volume as shown in Fig. 10(b) and a corresponding reduction in spectrum spread is observed as in Fig. 10(c). However a slight enhancement in spectrum spread for active layer volume less than $9.2\text{E} - 11\text{ cm}^3$ may be attributed to optical mode spillover phenomena that effectively increase the active layer volume more than the actual physical volume [21].

4.4. Comparison of the basic IM-DD system models

The most significant components appearing on RF spectrum are the detected carriers f_1 and f_2 , IMP-1025, HD-IMP-1000 and HD-1050 MHz besides many other less significant components. The present section aims to observe the influence of laser quantum efficiency, active layer volume and carrier life time on these components in the four basic IMDD systems.

4.4.1. System response to laser quantum efficiency

The collective observation of the detected carriers and distortion components are shown in Fig. 11(a)–(d) with respect to quantum efficiency ranging from 0 to 1. It is observed that with

increase in quantum efficiency all the detected carriers as well as the distortion components increase gradually with same gradient in each case. Also the power level difference between detected carriers and the distortion components is more pronounced in clipping disabled than in clipping enabled systems which have been realized by passing higher bias currents of order of 50 mA through the laser.

4.4.2. System response to active layer volume

The detected carriers and distortion components are plotted in Fig. 12(a)–(d) with respect to laser active layer volume varied from $5\text{E} - 11$ to $2.4\text{E} - 10\text{ cm}^3$. It is observed that both IMD and HD mechanisms are suppressed in lasers with small active layer volume and for lasers with large active layer volume these mechanisms are more pronounced till these achieve same power level as that of detected carriers. The dependence of IMPs and HD on active layer volume may be explained from the fact [21] that the threshold current density reduces with reduction in active layer volume so that the same carrier injection levels can be obtained with smaller drive currents and also the internal quantum efficiency increases, and suppresses the nonlinearities.

Additionally the HD components and the IMPs are of lower values in clipping disabled than in clipping enabled systems.

4.4.3. System response to laser carrier lifetime

With carrier lifetime varied from $8.842\text{E} - 10$ to $2\text{E} - 09\text{ s}$, the detected carriers in each IM-DD system are plotted in Fig. 13(a)–(d). It is observed that laser carrier life time value lower than $1.10\text{E} - 09\text{ s}$ results in much reduced detected power level whereas above this value detected carrier power level remains constant while distortion power levels reduce. Here also lower values of the HD components and IMPs are observed in clipping disabled than in clipping enabled system models. The power of detected carriers and distortion components have been noted in Table 2 at quantum efficiency equal to 0.4, laser active layer volume equal to $1.5\text{E} - 10\text{ cm}^3$ and the carrier

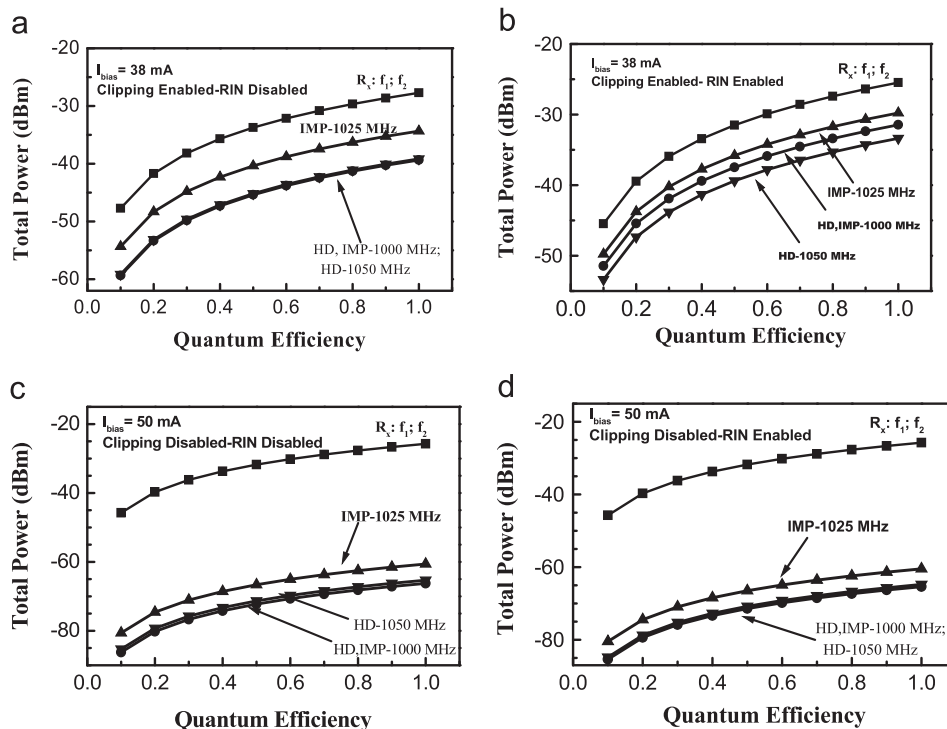


Fig. 11. Total power vs. quantum efficiency in case of (a) clipping enabled–RIN disabled, (b) clipping enabled–RIN enabled, (c) clipping disabled–RIN disabled, and (d) clipping disabled–RIN enabled.

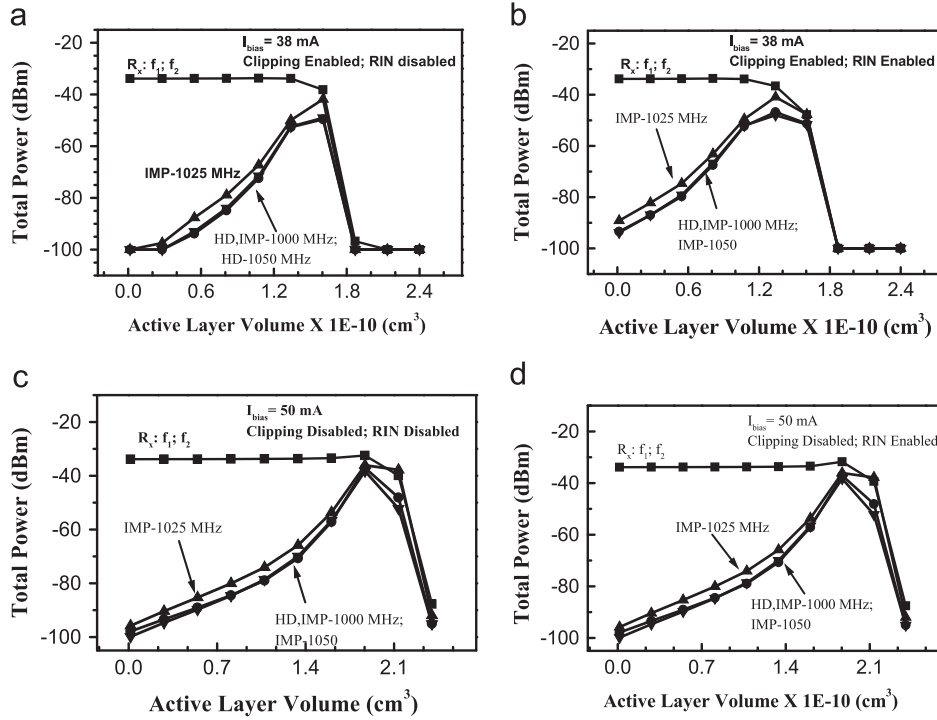


Fig. 12. Total power vs. laser active layer volume in case of (a) clipping enabled–RIN disabled, (b) clipping enabled–RIN enabled, (c) clipping disabled–RIN disabled, and (d) clipping disabled–RIN enabled.

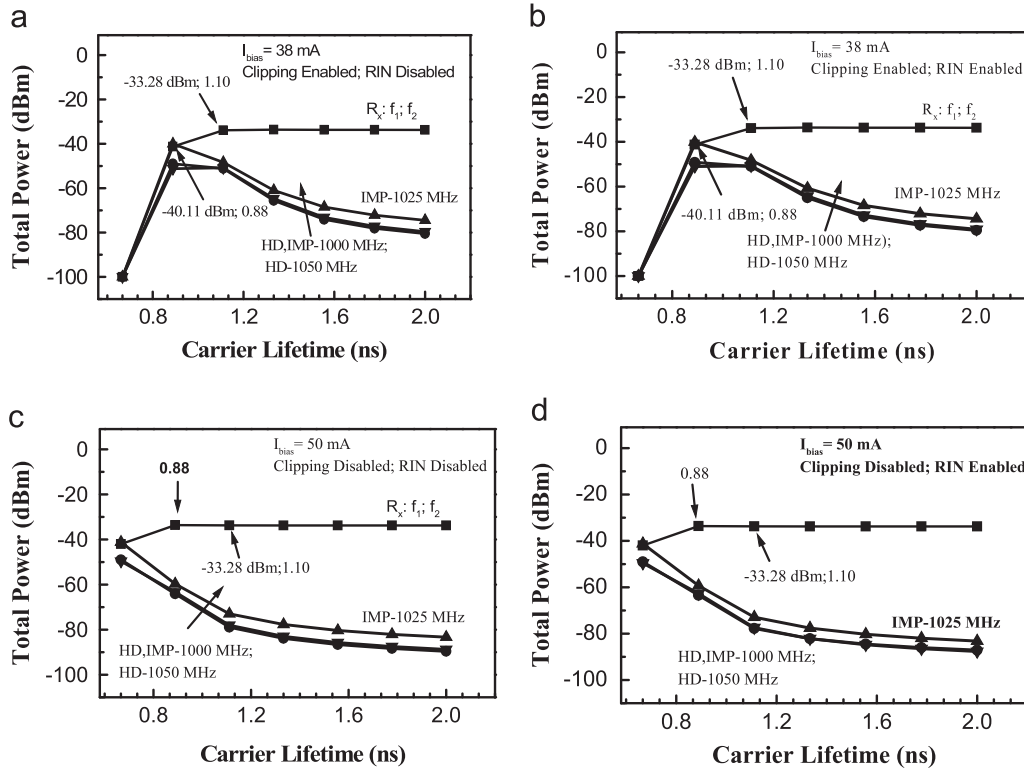


Fig. 13. Total power vs. laser carrier life time in case of (a) clipping enabled–RIN disabled (b) clipping enabled–RIN enabled (c) clipping disabled–RIN disabled, and (d) clipping disabled–RIN enabled.

lifetime $1E-9$ s. The power difference δ_{max} between detected carriers and the highest distortion component IMP-1025 is also noted in this table. The difference between detected carrier power and the highest distortion component IMP-1025 MHz is 6.53, 4.36, 35.54 and 34.59 dB in the four systems, respectively.

5. Conclusion and future scope

In this paper four basic IM-DD system models devised reveals distinct unique characteristics in the spectral domain that can be associated with the various impairment mechanisms influencing

Table 2
Power level of detected components in the four basic IM-DD systems.

Detected component at laser quantum efficiency of 0.4	Clipping enabled–RIN disabled (dBm)	Clipping enabled–RIN enabled (dBm)	Clipping disabled–RIN disabled (dBm)	Clipping disabled–RIN enabled (dBm)
Rx f_1f_2	–35.55	–33.38	–33.39	–33.54
IMP-1025	–42.08	–37.74	–68.93	–68.13
HD, IMP-1000	–47.19	–39.70	–74.14	–72.17
HD-1050	–47.19	–41.24	–73.60	–72.17
δ_{\max}	6.53	4.36	35.54	34.59

the respective system. The behaviour of Clipping and RIN noise mechanisms in the spectral domain as well, their impact on HD and IMD mechanisms active in these models have been investigated. The response of Clipping and RIN to system signal and device changes can be exploited in the direction of achieving better system performance.

RF spectrum display shows HD components in a single-tone clipping disabled–RIN disabled model, distinct IMP cluster group created in two-tone clipping disabled–RIN disabled model, clipping induced spillover in a two-tone clipping enabled–RIN disabled model, typical RIN spectrum in a two-tone clipping disabled–RIN enabled model and a RIN spectrum with clipping induced spillover in a two-tone clipping enabled–RIN enabled model, respectively. In a clipping enabled–RIN disabled system the clipping induced spectrum spillover bears a direct and moderately sensitive relationship with respect to modulation peak current and laser quantum efficiency and direct and highly sensitive relationship with respect to laser active layer. On the other hand it bears an inverse and highly sensitive relationship with respect to both laser bias current and carrier life time. In a clipping disabled–RIN enabled system the RIN spectrum does not show any sensitivity to changes in carrier amplitude, implying that laser RIN does not prove to be critical in selecting the modulation depth of the subcarriers. The RIN spectrum peak position shows a direct and moderately sensitive dependence on laser bias current, total insensitivity to laser quantum efficiency and inverse and highly sensitive dependence on laser active layer volume, respectively. The RIN spectrum peak power shows an inverse, uneven and moderately sensitive dependence on laser bias current and a direct and highly sensitive dependence on both laser quantum efficiency and laser active layer volume. The RIN spectrum width shows a direct, uneven and moderately sensitive dependence on laser bias current and quantum efficiency respectively and an inverse, uneven and highly sensitive dependence on active layer volume. Thus selection of higher bias current till permissible levels proves to be favorable to increase the immunity of the IMDD system to the negative influence of clipping and it would reasonably shift the RIN spectrum away from the usually used subcarrier frequencies in IMDD systems. However RIN spectrum will be spread over a large range in frequency domain. Lasers with low quantum efficiency are favorable for suppression of clipping and RIN

induced distortion. With active layer volume there will exist a tradeoff between clipping spillover and RIN related peak power on one hand and RIN related peak position and spectral width on the other hand. High carrier lifetime should be selected to reduce the clipping spillover. However the final selection of a particular carrier life time has to take into account other factors dependent on this parameter like the laser radiation recombination coefficient and carrier diffusion lengths.

The comparative study based on these models reveals the clipping enabled–RIN enabled system model as the worst case IM-DD model with the least power gap between detected carriers and distortion component and hence will suffer from maximum negative influence of the prevalent distortion in the system. Also the clipping disabled–RIN disabled is most favourable of the IMDD systems with the widest power gap and hence would suffer least from the negative influence of the distortion.

This work deals with the device linearity and noise requirements in a directly modulated IM-DD-SCM system models which are under the influence of clipping, RIN and their impact on HD and IMD mechanisms. This study would lead to simplification in terms of selecting a source, or operational characteristics and administering the network. In future the four models so devised can be further investigated analytically and their performance under different modulation format studied.

References

- [1] Yuichi Tanka, A Study on Optical Wireless Communication System and their Applications, Ph.D. Thesis, Keio University, Japan, 2002.
- [2] Hejie Yang, Optical Techniques for Broadband In-building Networks, Ph.D. Thesis, Department of Electrical Engineering, Technische Universiteit Eindhoven, 2011.
- [3] R. Olshansky, V.A. Lanzisera, *Electron. Lett* 23 (1987) 1196.
- [4] Robert Olshansky, Vincent A. Lanzisera, Paul M. Hill, *J. Lightwave Technol* 7 (1989) 1329.
- [5] Su Li, UWB Radio-over-Fiber System Using Directly Modulated VCSEL, Thesis for Master of Applied Science in Electrical and Computer Engineering, University of Waterloo, Canada, 2007.
- [6] Vishal Sharma, Amarपाल Singh, Ajay K. Sharma, *Opt. Lasers Eng* 47 (2009) 1145.
- [7] Vishal Sharma, Amarपाल Singh, Ajay K. Sharma, *Optik* 121 (2010) 1545.
- [8] Mukesh Kumar, Sandeep Singh, Jay Singh, Rohini Saxena, *IJARCSSE* 6 (2012) 112.
- [9] Thomas E. Darcie, *IEEE J. Sel. Areas Commun* 8 (1990) 1240.
- [10] Rajappa Papaannareddy, George Bodeep, HFC/CATV Transmission System, (Invited Paper), Purdue University, Westville, USA, 2002.
- [11] S. Betti, E. Bravi, M. Giaconi, *Comput. Network* 32 (2000) 563.
- [12] T.E. Darcie, P.P. Iannone, B.L. Kasper, J.R. Talman, C.A. Burrus, T.A. Baker, *J. Lightwave Technol.* 7 (1989) 997.
- [13] L. Roselli, V. Borgioni, F. Zepparelli, M. Ambrosi, M. Comez, P. Faccin, A. Casini, *J. Lightwave Technol.* 21 (2003) 1211.
- [14] S. Chandra, P.K. Chaturvedi, *IEEE* (2005) 540.
- [15] Attilio J. Rainal, *J. Lightwave Technol* 14 (1996) 474.
- [16] Anthony Leung, Performance Analysis of SCM Optical Transmission Link for Fiber-to-the-Home, Master of Science Thesis, Department of Electrical Engineering & Computer Science, University of Kansas, 2004.
- [17] T.E. Darcie, M.E. Dixon, B.L. Kasper, C.A. Burrus, *Electron. Lett.* 22 (1986) 774.
- [18] Govind P. Agrawal, *Fiber-optic Communication System*, third ed., Wiley-Interscience, A John Wiley & Sons.
- [19] John M. Senior, M. Yousif Jamro, *Optical fiber communication, principles and practice*, third ed., Prentice Hall, Pearson, 2009.
- [20] OptiSystem Simulator. V9, Canada.
- [21] Pallab Bhattacharya, *Semiconductor Optoelectronic Devices*, second ed., Prentice Hall, Pearson, 2008.